Optimal Parameter Estimation with Homogeneous Entities and Arbitrary Constraints

Jochen Meidow[1], Wolfgang Förstner[2], and Christian Beder

[1] Research Institute for Optronics and Pattern Recognition, Ettlingen, Germany
meidow@fom.fgan.de
[2] Institute for Geodesy and Geoinformation, University of Bonn, Germany
wf@ipb.uni-bonn.de

Abstract. Well known estimation techniques in computational geometry usually deal only with single geometric entities as unknown parameters and do not account for constrained observations within the estimation.
The estimation model proposed in this paper is much more general, as it can handle multiple homogeneous vectors as well as multiple constraints. Furthermore, it allows the consistent handling of arbitrary covariance matrices for the observed and the estimated entities. The major novelty is the proper handling of singular observation covariance matrices made possible by additional constraints within the estimation. These properties are of special interest for instance in the calculus of algebraic projective geometry, where singular covariance matrices arise naturally from the non-minimal parameterizations of the entities.
The validity of the proposed adjustment model will be demonstrated by the estimation of a fundamental matrix from synthetic data and compared to heteroscedastic regression [1], which is considered as state-of-the-art estimator for this task. As the latter is unable to simultaneously estimate multiple entities, we will also demonstrate the usefulness and the feasibility of our approach by the constrained estimation of three vanishing points from observed uncertain image line segments.

1 Introduction

The final step in uncertain geometric reasoning usually is the optimal estimation of unknown parameters from given uncertain observations taking geometric or algebraic constraints into account, which either result from the structure of the problem or have been found by some hypothesis generation process, e.g. [2–4].

The well known estimation techniques in geometric computation (e.g. [1, 5–7]) usually deal only with single homogeneous entities, for instance points or transformations. These estimation techniques, such as algebraic minimization, total least squares, renormalization, or heteroscedastic regression cannot easily be generalized to the estimation of multiple homogeneous entities with multiple constraints, which is necessary in many vision tasks for instance when dealing

with composed geometric entities such as straight line segments or the joint estimation of vanishing points.

In order to address this problem we provide a generic estimation model for the simultaneous estimation of more than one uncertain geometric entity. Based on possibly correlated observed geometric entities, the results are derived in consideration of constraints for the parameters and the observations. In particular the proposed procedure is able to handle uncertain homogeneous vectors together with possibly singular covariance matrices extending the hitherto known techniques w.r.t. the continuous use of homogeneous representations.

To demonstrate the applicability of the proposed estimation scheme we show how the presented general estimation framework can be specialized for two exemplary vision tasks. First, we demonstrate the applicability of our approach for the very well-known and well-understood task of estimating the fundamental matrix from uncertain homogeneous point correspondences. We show, that competitive results are achieved by comparing our approach to heteroscedastic regression [1], which is considered as state-of-the-art estimator for this task. Second, we show how three orthogonal vanishing points can be estimated simultaneously from uncertain straight line segments in homogeneous representation for a real scene using the proposed framework. In contrast to other estimation techniques (e.g. [1, 5–7]), our approach is directly applicable for this task and no re-parameterization is required due to the rigorous handling of the singular uncertainty structure of the homogeneous entities. Therefore, the presented framework can directly benefit from the compact representation of many vision problems using algebraic projective geometry, so that the task of formulating estimation schemes is greatly simplified.

2 General Adjustment Model with Constraints

We will start by presenting the general problem-specific modeling tasks before we will give examples for two specific vision tasks in Sect. 3. The approach is based on the adjustment model proposed in [8]. The model consists of a functional part for the unknown parameters and the observations, a stochastic part for the observations, an objective function, and an iterative estimation procedure for non-linear problems.

2.1 Mathematical Model

Functional model. The functional model describes the mutual relations between the considered entities comprising of the observations and the parameters to be estimated. We distinguish three types of constraints between the true observations $\widetilde{\boldsymbol{l}}$ and the U unknown true parameters $\widetilde{\boldsymbol{p}}$:

1. the G conditions $\boldsymbol{g}(\widetilde{\boldsymbol{l}}, \widetilde{\boldsymbol{p}}) = \mathbf{0}$ between the observations and parameters reflecting their actual intended mutual relation (i.e. the model assumptions),

2. the H restrictions $\boldsymbol{h}(\widetilde{\boldsymbol{p}}) = \boldsymbol{0}$ on the parameters alone reflecting intrinsic constraints (e.g. $||\widetilde{\boldsymbol{p}}|| = 1$ for homogeneous entities) and enabling singular parameter covariance matrices, and finally
3. the C constraints $\boldsymbol{c}(\widetilde{\boldsymbol{l}}) = \boldsymbol{0}$ on the observations alone reflecting intrinsic constraints (e.g. $||\widetilde{\boldsymbol{l}}|| = 1$ for homogeneous entities) and enabling singular observation covariance matrices.

The error-free observations $\widetilde{\boldsymbol{l}}$ are related to the real observations $\boldsymbol{l}$ by additive unknown corrections $\widetilde{\boldsymbol{l}} = \boldsymbol{l} + \widetilde{\boldsymbol{v}}$. Since the true values remain unknown they will be replaced by their estimates $\widehat{\boldsymbol{p}}$, $\widehat{\boldsymbol{l}}$ and $\widehat{\boldsymbol{v}}$ in the following.

Stochastic model. The stochastic model describes the uncertainty of the observations. An initial covariance matrix $\boldsymbol{\Sigma}_{ll}^{(0)}$ of the observations is assumed to be known which subsumes the stochastic properties of the observations, thus $\boldsymbol{l}$ is assumed to be normally distributed $\boldsymbol{l} \sim N(\widetilde{\boldsymbol{l}}, \widetilde{\boldsymbol{\Sigma}}_{ll})$. With the possibly unknown variance factor σ_0^2, the matrix $\boldsymbol{\Sigma}_{ll}^{(0)}$ is related to the true covariance matrix $\widetilde{\boldsymbol{\Sigma}}_{ll}$ by $\boldsymbol{\Sigma}_{ll} = \sigma_0^2 \boldsymbol{\Sigma}_{ll}^{(0)}$ (cf. [9]). Note, that we explicitly allow $\boldsymbol{\Sigma}_{ll}$ to be singular as long as its null space is properly handled by the constraint $\boldsymbol{c}(\widetilde{\boldsymbol{l}}) = \boldsymbol{0}$. This is one of the major contributions of this work.

Having defined the problem specific model (see Sect. 3 for examples, how this framework can be specialized to specific vision problems), we will now derive a corresponding estimation scheme for estimating the parameters and the adjusted observations in the next section. We will also show how the unknown variance factor σ_0^2 can be estimated from the estimated corrections $\widehat{\boldsymbol{v}}$, i.e. the negative residuals.

2.2 Objective Function and Estimation

Finding optimal estimates $\widehat{\boldsymbol{p}}$ and $\widehat{\boldsymbol{l}}$ for $\boldsymbol{p}$ and $\boldsymbol{l}$ resp. can be done by minimizing the weighted squared residuals subject to the given constraints, i.e.

$$L(\widehat{\boldsymbol{v}}, \widehat{\boldsymbol{p}}, \boldsymbol{\lambda}, \boldsymbol{\mu}, \boldsymbol{\nu}) = \frac{1}{2} \widehat{\boldsymbol{v}}^{\mathsf{T}} \boldsymbol{\Sigma}_{ll}^{+} \widehat{\boldsymbol{v}} + \boldsymbol{\lambda}^{\mathsf{T}} \boldsymbol{g}(\boldsymbol{l} + \widehat{\boldsymbol{v}}, \widehat{\boldsymbol{p}}) + \boldsymbol{\mu}^{\mathsf{T}} \boldsymbol{h}(\widehat{\boldsymbol{p}}) + \boldsymbol{\nu}^{\mathsf{T}} \boldsymbol{c}(\boldsymbol{l} + \widehat{\boldsymbol{v}}) \quad (1)$$

with the Lagrangian vectors $\boldsymbol{\lambda}$, $\boldsymbol{\mu}$ and $\boldsymbol{\nu}$. In contrast to [2] we explicitly include the constraint $\boldsymbol{c}(\boldsymbol{l}+\widehat{\boldsymbol{v}})$ in order to properly deal with singular covariance matrices consistent with the pseudo-inverse $\boldsymbol{\Sigma}_{ll}^{+}$ (see [8] for details).

For solving this non-linear problem in an iterative manner we need approximate values $\widehat{\boldsymbol{p}}^{(0)}$ and $\widehat{\boldsymbol{l}}^{(0)}$ for the estimates of the unknown parameters $\widehat{\boldsymbol{p}} = \widehat{\boldsymbol{p}}^{(0)} + \widehat{\Delta \boldsymbol{p}}$ and $\widehat{\boldsymbol{l}} = \widehat{\boldsymbol{l}}^{(0)} + \widehat{\Delta \boldsymbol{l}} = \boldsymbol{l} + \widehat{\boldsymbol{v}}$. The corrections $\widehat{\Delta \boldsymbol{p}}$ for the unknowns and the estimated observations $\widehat{\boldsymbol{l}}$ are obtained iteratively by applying the following steps (see [8] for a detailed derivation of the estimation formulas):

1. The Jacobians are computed at the current approximate values

$$\boldsymbol{A} = \frac{\partial \boldsymbol{g}(\boldsymbol{l}, \boldsymbol{p})}{\partial \boldsymbol{p}}, \quad \boldsymbol{B}^{\mathsf{T}} = \frac{\partial \boldsymbol{g}(\boldsymbol{l}, \boldsymbol{p})}{\partial \boldsymbol{l}}, \quad \boldsymbol{C}^{\mathsf{T}} = \frac{\partial \boldsymbol{c}(\boldsymbol{l})}{\partial \boldsymbol{l}}, \quad \boldsymbol{H}^{\mathsf{T}} = \frac{\partial \boldsymbol{h}(\boldsymbol{p})}{\partial \boldsymbol{p}} \quad (2)$$

2. In each iteration τ compute the approximate values for the residuals of the constraints

$$\boldsymbol{g}_\tau = \boldsymbol{g}(\boldsymbol{l}^{(\tau)}, \boldsymbol{p}^{(\tau)}), \qquad \boldsymbol{h}_\tau = \boldsymbol{h}(\boldsymbol{p}^{(\tau)}), \qquad \boldsymbol{c}_\tau = \boldsymbol{c}(\boldsymbol{l}^{(\tau)}) \tag{3}$$

3. Compute the auxiliary variable

$$\boldsymbol{a} = \boldsymbol{B}^\mathsf{T}\boldsymbol{C}(\boldsymbol{C}^\mathsf{T}\boldsymbol{C})^{-1}(\boldsymbol{C}^\mathsf{T}(\boldsymbol{l} - \boldsymbol{l}^{(\tau)}) + \boldsymbol{c}_\tau) - \boldsymbol{B}^\mathsf{T}(\boldsymbol{l} - \boldsymbol{l}^{(\tau)}) - \boldsymbol{g}_\tau \tag{4}$$

4. Compute the covariance matrix $\boldsymbol{\Sigma}_{gg} = \boldsymbol{B}^\mathsf{T}\boldsymbol{\Sigma}_{ll}\boldsymbol{B}$ of the contradictions $\boldsymbol{g}_\tau$
5. The unknown corrections to the parameters are now computed by solving the normal equation system

$$\begin{bmatrix} \boldsymbol{A}^\mathsf{T}\boldsymbol{\Sigma}_{gg}^{-1}\boldsymbol{A} & \boldsymbol{H} \\ \boldsymbol{H}^\mathsf{T} & \boldsymbol{0} \end{bmatrix} \begin{bmatrix} \widehat{\boldsymbol{\Delta p}} \\ \boldsymbol{\mu} \end{bmatrix} = \begin{bmatrix} \boldsymbol{A}^\mathsf{T}\boldsymbol{\Sigma}_{gg}^{-1}\boldsymbol{a} \\ -\boldsymbol{h}_\tau \end{bmatrix}. \tag{5}$$

6. The Lagrangians and the residuals are finally computed as

$$\boldsymbol{\lambda} = \boldsymbol{\Sigma}_{gg}^{-1}(\boldsymbol{A}\widehat{\boldsymbol{\Delta p}} - \boldsymbol{a}) \tag{6}$$

$$\widehat{\boldsymbol{v}}^{(\tau)} = -\boldsymbol{\Sigma}_{ll}\boldsymbol{B}\boldsymbol{\lambda} - \boldsymbol{C}(\boldsymbol{C}^\mathsf{T}\boldsymbol{C})^{-1}(\boldsymbol{C}^\mathsf{T}(\boldsymbol{l} - \boldsymbol{l}^{(\tau)}) + \boldsymbol{c}_\tau) \tag{7}$$

The approximate values have to be iteratively improved for non-linear problems. In doing so, the covariance matrix $\boldsymbol{\Sigma}_{ll}^{(\tau)}$ of the observations have to be adjusted within each iteration step to be consistent with the constraint $\boldsymbol{c}(\boldsymbol{l}^{(\tau)} + \widehat{\boldsymbol{v}})$, e.g. by spherical normalization, because of the change of the observations $\boldsymbol{l}^{(\tau)}$ within the iteration process. Note, that the estimation procedure is not problem specific except for the computation of the Jacobians in the first step and can be applied in a black-box manner.

2.3 Precision of the Estimates

One of the advantages of uncertainty modeling is the possibility of propagating errors. We will now show, how the precision of the estimated parameters can be derived. With estimated corrections $\widehat{\boldsymbol{v}}$ from (7) we obtain the fitted observations $\widehat{\boldsymbol{l}} = \boldsymbol{l} + \widehat{\boldsymbol{v}}$. The estimation for the variance factor σ_0^2 is given by the maximum likelihood estimation $\widehat{\sigma}_0^2 = \widehat{\boldsymbol{v}}^\mathsf{T}\boldsymbol{\Sigma}_{ll}^{+}\widehat{\boldsymbol{v}}/R$ with the redundancy $R = G + H - U$, cf. [9]. The pseudo inverse can eventually efficiently computed by exploiting the block diagonal matrix structures and the relation $\boldsymbol{C}^\mathsf{T}\boldsymbol{C} = \boldsymbol{I}$ (cf. the examples in Sect. 3).

We finally obtain the estimated covariance matrix $\widehat{\boldsymbol{\Sigma}}_{\widehat{pp}} = \widehat{\sigma}_0^2\boldsymbol{\Sigma}_{\widehat{pp}}$ of the estimated parameters, where $\boldsymbol{\Sigma}_{\widehat{pp}}$ results from the inverted reduced normal equation matrix by variance propagation:

$$\begin{bmatrix} \boldsymbol{\Sigma}_{\widehat{pp}} & \cdot \\ \cdot & \cdot \end{bmatrix} = \begin{bmatrix} \boldsymbol{A}^\mathsf{T}\boldsymbol{\Sigma}_{gg}^{-1}\boldsymbol{A} & \boldsymbol{H} \\ \boldsymbol{H}^\mathsf{T} & \boldsymbol{O} \end{bmatrix}^{-1} \tag{8}$$

Observe, the model has the same structure as the classical Gauss-Markov-model with constraints [9], which allows to easily modify for a robust ML-type estimation to cope with outliers [10] by iteratively reweighting the individual conditions g_i.

3 Examples

Having derived a very generic modeling and estimation framework in the previous section we will now show, how the presented framework can be specialized for two exemplary vision problems.

3.1 Estimation of the Fundamental Matrix

As a first exemplary problem we consider the very well-known and well-understood problem of fundamental matrix estimation from uncertain image point correspondences. Since the 3×3 fundamental matrix $\mathbf{F}$ is homogeneous and singular, two constraints have to be introduced for the 9 elements $\mathbf{f} = \mathrm{vec}(\mathbf{F})$.

With at least 7 corresponding point pairs captured by straight-line preserving cameras the fundamental matrix can be estimated from the coplanarity constraints

$$\mathbf{x}_i'^{\mathsf{T}} \mathbf{F} \mathbf{x}_i'' = (\mathbf{x}_i''^{\mathsf{T}} \otimes \mathbf{x}_i'^{\mathsf{T}}) \mathbf{f} = 0 \tag{9}$$

which are bilinear in the corresponding homogeneous image coordinates $\mathbf{x}_i'$ and $\mathbf{x}_i''$, and linear in the elements of the fundamental matrix. Suitable constraints for the observations and for the parameters are

$$\mathbf{x}_i^{\mathsf{T}} \mathbf{x}_i - 1 = 0, \qquad \mathbf{f}^{\mathsf{T}} \mathbf{f} - 1 = 0, \qquad \text{and} \qquad \det(\mathbf{F}) = 0, \tag{10}$$

fixing the scale factors and enforcing the rank two constraint.

With the covariance matrix $\boldsymbol{\Sigma}_{xx}$ of the Euclidean coordinates $\boldsymbol{x} = [x, y]^{\mathsf{T}}$ of an image point the initial representation is $\mathbf{x} = [\boldsymbol{x}^{\mathsf{T}}, 1]^{\mathsf{T}}$ and $\boldsymbol{\Sigma}_{\mathrm{xx}} = \mathrm{Diag}(\boldsymbol{\Sigma}_{xx}, 0)$ assuming the factor of proportionality to be non stochastic. Spherical normalization leads to the observations $\mathbf{x} := \mathbf{x}/|\mathbf{x}|$ with $\boldsymbol{\Sigma}_{\mathrm{xx}} := \boldsymbol{J} \boldsymbol{\Sigma}_{\mathrm{xx}} \boldsymbol{J}^{\mathsf{T}}$ using the Jacobian

$$\boldsymbol{J} = \frac{1}{|\mathbf{x}|} \left(\boldsymbol{I}_3 - \frac{\mathbf{x}\mathbf{x}^{\mathsf{T}}}{\mathbf{x}^{\mathsf{T}}\mathbf{x}} \right) \tag{11}$$

for each point. For n image points the vector of observations is $\boldsymbol{l} = [\mathbf{x}_1^{\mathsf{T}}, \mathbf{x}_2^{\mathsf{T}}, \ldots, \mathbf{x}_n^{\mathsf{T}}]^{\mathsf{T}}$ and the corresponding covariance matrix $\boldsymbol{\Sigma}_{ll} = \mathrm{Diag}(\boldsymbol{\Sigma}_{\mathrm{x}_1\mathrm{x}_1}, \boldsymbol{\Sigma}_{\mathrm{x}_2\mathrm{x}_2}, \ldots, \boldsymbol{\Sigma}_{\mathrm{x}_n\mathrm{x}_n})$. Observe, we introduce all constraints at once, and in contrast to classical approaches may use the uncertain homogeneous entities directly, without the need for special treatment of the last coordinate.

The Jacobian of the n coplanarity constraints (9) is $\boldsymbol{A} = [\mathbf{x}_1'' \otimes \mathbf{x}_1', \mathbf{x}_2'' \otimes \mathbf{x}_2', \ldots, \mathbf{x}_n'' \otimes \mathbf{x}_n']^{\mathsf{T}}$ where $\otimes$ denotes the Kronecker product and the singular value decomposition (SVD) of $\boldsymbol{A}$ yields the approximate values for the parameters $\mathbf{f}$. Furthermore, by considering the SVD of $\mathbf{F}$ the rank two property can be enforced [11].

The Jacobians of (9) and (10) are $\boldsymbol{B} = \mathrm{Diag}([\mathbf{x}_1''^{\mathsf{T}}\mathbf{F}^{\mathsf{T}}, \mathbf{x}_1'^{\mathsf{T}}\mathbf{F}], [\mathbf{x}_2''^{\mathsf{T}}\mathbf{F}^{\mathsf{T}}, \mathbf{x}_2'^{\mathsf{T}}\mathbf{F}], \ldots)$, $\boldsymbol{A}$, $\boldsymbol{C} = 2\ \mathrm{Diag}(\mathbf{x}_1', \mathbf{x}_1'', \ \mathbf{x}_2', \mathbf{x}_2'', \ \ldots, \mathbf{x}_n', \mathbf{x}_n'')$, and $\boldsymbol{H} = [2\mathbf{f}, \mathbf{f}^*]^{\mathsf{T}}$, where $\mathbf{f}^* = \mathrm{vec}(\mathbf{F}^*)$ denotes the elements of the adjoint $\mathbf{F}^*$ of $\mathbf{F}$. Since $\boldsymbol{C}^{\mathsf{T}}\boldsymbol{C} = \boldsymbol{I}$ holds, the pseudo inverse of $\boldsymbol{\Sigma}_{ll}$ can efficiently be computed by $\boldsymbol{\Sigma}_{ll}^{+} = (\boldsymbol{\Sigma}_{ll} + \boldsymbol{C}\boldsymbol{C}^{\mathsf{T}})^{-1} - \boldsymbol{C}\boldsymbol{C}^{\mathsf{T}}$ exploiting the block diagonal matrix structures.

To validate the adjustment model we performed the following stochastic simulation: In 500 simulation runs we generated 50 3d points, each with normal distributed coordinates. The two camera orientations have been randomly selected with camera centers on a sphere with radius 6 around the point cloud and viewing directions toward the center of the point cloud. This leads to observed image coordinates in the range of approximately $[-1, 1]$. After adding isotropic noise with $\sigma_n = 0.02$ to the Euclidean image coordinates the parameters of the fundamental matrix have been estimated assuming i.i.d. observations.

The Mahalanobis distance between the estimated and the true values $\mathbf{f}$ is computed for each of the simulation runs. Figure 1 shows the empirical distribution of the Mahalanobis distance which is χ^2 distributed with 7 degrees of freedom as expected. The hypothesized inequality of both distributions has been rejected by the Kolmogorov-Smirnov goodness-of-fit test at significance level $\alpha = 0.05$.

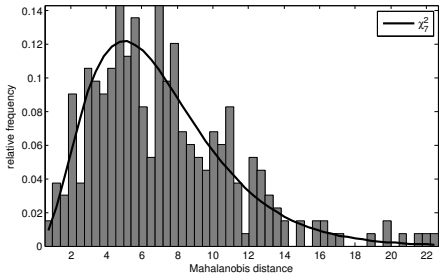

		8-point	HEIV	our approach
singular values	σ_1/σ_2	0.0323	0.0290	0.0288
1st epipole	x_1	0.0775	0.0585	0.0591
	y_1	0.0808	0.0645	0.0631
2nd epipole	x_2	0.0737	0.0633	0.0638
	y_2	0.0798	0.0701	0.0703

Fig. 1. Right: Empirical distribution of the Mahalanobis distance and its theoretical χ^2_7-distribution. Left: Comparison of the estimation results. Robust estimation of the standard deviations of the parameters by the median absolute deviation w.r.t. the true values.

To assess and compare the results we choose the HEIV based estimation [1] as a representative for competing state-of-the-art estimators. For the HEIV estimation the implementation [12] has been used. Figure 1 shows the results for the estimation of the coordinates of the epipoles and the ratio of the estimated singular values for the eight point algorithm, the HEIV, and our approach. For the estimated parameters, the stated values denote a robust estimation of the standard deviation by computing the median absolute deviation of the residuals w.r.t. the true values, multiplied by 1.4826. According to the achieved precisions, the results of the HEIV based estimation and our approach are the same up to numerical effects due to the number of iterations.

3.2 Constrained Vanishing Points Determination

As a second example we chose the task of joint vanishing point estimation using all available constraints. In contrast to the computation of the fundamental

matrix demonstrated in the previous section, the HEIV algorithm cannot be generalized easily to solve this task due to the multiple constraints on the estimated entities. Since a vanishing point may lie at infinity, the use of the homogeneous representation is a reasonable choice.

Figure 2 shows on the left side the first image of the corridor sequence with extracted straight line segments provided by the Visual Geometry Group, University of Oxford. By using a random sample consensus [13] the segments have been classified according to the 3 vanishing directions and an outliers class.

Fig. 2. First image of the Oxford corridor sequence. Left: Extracted straight line segments, classified according to their vanishing directions and an outlier class. Right: Display detail with superimposed confidence regions, the approximate third vanishing point ($\circ$), and its estimation ($+$).

For each of the three sets of straight line segments the corresponding n_k straight lines $\mathbf{l}_{ki}$ should intersect in the vanishing point $\mathbf{v}_k$, not to be confused with the residual vector $\boldsymbol{v}$. Thus the constraints are

$$\mathbf{v}_k^\mathsf{T}\mathbf{l}_{ki} = 0, \quad \mathbf{v}_k^\mathsf{T}\mathbf{v}_k - 1 = 0, \quad \mathbf{l}_{ki}^\mathsf{T}\mathbf{l}_{ki} - 1 = 0, \quad k = 1\ldots 3,\ i = 1\ldots n_k \tag{12}$$

because of the incidences and the spherical normalizations of the geometric entities. Furthermore, if the homogeneous calibration matrix $\mathbf{K}$ for the straight line preserving camera is known, we can introduce the two additional constraints

$$\mathbf{v}_1^\mathsf{T}\omega\mathbf{v}_2 = 0 \qquad \text{and} \qquad \mathbf{v}_2^\mathsf{T}\omega\mathbf{v}_3 = 0 \tag{13}$$

which hold because of the orthogonality relations of the three vanishing directions $\mathbf{K}^{-1}\mathbf{v}_k$ and where $\omega = \mathbf{K}^{-\mathsf{T}}\mathbf{K}^{-1}$ denotes the image of the absolute conic [11].

The straight line segments are given without any information about their uncertainty. Therefore, we initially determined the covariance matrices $\boldsymbol{\Sigma}_{a_i a_i}$ and

$\boldsymbol{\Sigma}_{b_i b_i}$ of the coordinates of the segment end-points $\boldsymbol{a}_i$ and $\boldsymbol{b}_i$ with the help of the Förstner operator [14]. Then, assuming independent end-points, we determined each straight line $\mathbf{l}_i$ by joining the corresponding end-points accompanied by variance propagation [2]

$$\mathbf{l}_i = \boldsymbol{S}_{\mathrm{a}_i}\mathbf{b}_i, \qquad \boldsymbol{\Sigma}_{\mathrm{l}_i\mathrm{l}_i} = [-\boldsymbol{S}_{\mathrm{b}_i}, \boldsymbol{S}_{\mathrm{a}_i}]\,\mathrm{Diag}(\boldsymbol{\Sigma}_{\mathrm{a}_i\mathrm{a}_i}, \boldsymbol{\Sigma}_{\mathrm{b}_i\mathrm{b}_i})\,[-\boldsymbol{S}_{\mathrm{b}_i}, \boldsymbol{S}_{\mathrm{a}_i}]^{\mathsf{T}} \tag{14}$$

where $\boldsymbol{S}(\cdot)$ denotes the skew-symmetric matrix inducing the cross product. Thus, with all n straight lines the vector of observations is $\boldsymbol{l} = \left[\mathbf{l}_1^{\mathsf{T}}, \mathbf{l}_2^{\mathsf{T}}, \ldots, \mathbf{l}_n^{\mathsf{T}}\right]^{\mathsf{T}}$ and its covariance matrix $\boldsymbol{\Sigma}_{ll} = \mathrm{Diag}(\boldsymbol{\Sigma}_{\mathrm{l}_1\mathrm{l}_1}, \boldsymbol{\Sigma}_{\mathrm{l}_2\mathrm{l}_2}, \ldots, \boldsymbol{\Sigma}_{\mathrm{l}_n\mathrm{l}_n})$.

Figure 2 shows on the right side a detail of the image with superimposed straight line segments, the 99% confidence ellipses of the end-points enlarged by factor 10, and the resulting error hyperbolas of the corresponding straight lines.

Approximate values can easily be obtained by considering each vanishing point individually. The Jacobian of the constraints w.r.t. the unknown parameters is simply $\boldsymbol{A}_k = \left[\mathbf{l}_{k1}, \mathbf{l}_{k2}, \ldots \mathbf{l}_{kn}\right]^{\mathsf{T}}$, and the singular value decomposition of $\boldsymbol{A}_k$ yields the approximate values for the vanishing points $\mathbf{v}_k$.

For the joint parameter estimation with $n = n_1 + n_2 + n_3$ observed straight lines the block-diagonal Jacobians are

$$\begin{aligned} \boldsymbol{A} &= \mathrm{Diag}(\boldsymbol{A}_1, \boldsymbol{A}_2, \boldsymbol{A}_2) \\ \boldsymbol{B} &= \mathrm{Diag}(\boldsymbol{I}_{n_1} \otimes \mathbf{v}_1, \boldsymbol{I}_{n_2} \otimes \mathbf{v}_2, \boldsymbol{I}_{n_3} \otimes \mathbf{v}_3), \\ \boldsymbol{C} &= 2\mathrm{Diag}(\mathbf{l}_1, \mathbf{l}_2, \ldots, \mathbf{l}_n) \end{aligned} \quad \boldsymbol{H} = \begin{bmatrix} 2\mathbf{v}_1 & \mathbf{0} & \mathbf{0} & \omega\mathbf{v}_2 & \mathbf{0} \\ \mathbf{0} & 2\mathbf{v}_2 & \mathbf{0} & \omega\mathbf{v}_1 & \omega\mathbf{v}_3 \\ \mathbf{0} & \mathbf{0} & 2\mathbf{v}_3 & \mathbf{0} & \omega\mathbf{v}_2 \end{bmatrix}^{\mathsf{T}},$$

whereas $\otimes$ denotes the Kronecker product. Again, since $\boldsymbol{C}^{\mathsf{T}}\boldsymbol{C} = \boldsymbol{I}$ holds the pseudo inverse of $\boldsymbol{\Sigma}_{ll}$ can efficiently be computed by exploitation of the block diagonal matrix structures.

For the visual presentation of the estimation results we choose a gnomonic projection of the image and the three vanishing points, because this projection is suitable to represent the two vanishing points near infinity. For the projection we used a sphere with radius equal to the camera constant and the principal point of the camera as tangent point. Figure 3 shows the results with and without the orthogonality constraints (13).

For the visualisation of the confidence regions we generated normal distributed samples according to the estimates, e.g., $\mathbf{v} \sim N(\widehat{\mathbf{v}}, \widehat{\boldsymbol{\Sigma}}_{\widehat{\mathrm{v}}\widehat{\mathrm{v}}})$, in homogeneous representation and mapped them with the inverse calibration matrix $\mathbf{K}^{-1}$ to the sphere. As expected, the three orthogonal clusters follow Bingham's distribution [15]. Observe, that the inclusion of the orthogonality constraint into a joint estimation improves the accuracy as expected. Also note, that for the third vanishing point the 99% confidence region overlaps the equator (i.e. the corresponding image point is near infinity and therefore may lie on the opposite side in the image), which is handled by the use of uncertain homogeneous entities in a straightforward manner.

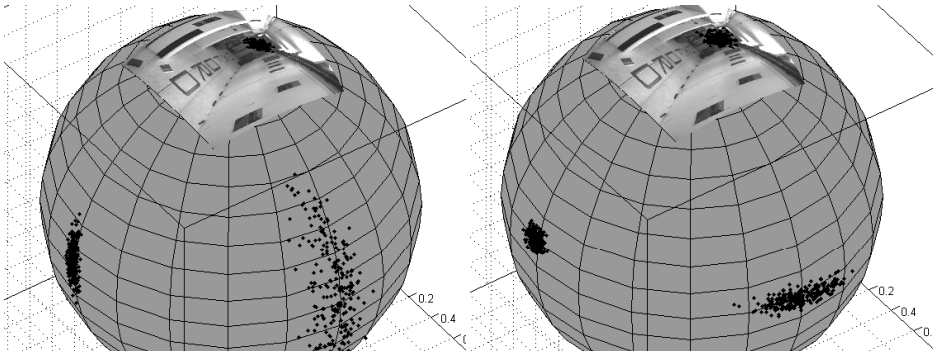

Fig. 3. Image and vanishing points in gnomonic projection. left side: without orthogonal constraints, right side: with additional constraints to enforce the directions to be mutually orthogonal. The 99% confidence regions of the vanishing directions follow Bingham's distribution and have been enlarged by a factor of 10.

4 Conclusions

We developed a scheme for simultaneous estimating sets of homogeneous entities from observed homogeneous entities with an arbitrary number of constraints and possible rank defect covariance matrices in order to integrate projective geometry and estimation theory.

The consideration of uncertainty and correlations of the observed entities leads to statistically optimal results as in the case of the equivalent Euclidean representation. Thereby, possibly singular covariance matrices of homogeneous entities can be treated. Since the model uses the same equations as for the unconstrained algebraic minimization, there is no need to change the representations during the geometric reasoning. The adjustment model is of special interest within the calculus of projective geometry, but the approach is not restricted to problems with normalization constraints for homogeneous entities.

The proposed adjustment model has been statistically validated with synthetic data and approved with real data sets. The results for the estimation of fundamental matrices based on synthetic data are comparable to the ones achieved by the heteroscedastic errors-in-variables (HEIV) approach being considered as a state-of-the-art estimator for such problems. The procedure can cope with considerably large noise of the point coordinates. The constrained estimation of vanishing points in a real image leads to statistically optimal results due to the stringent consideration of uncertainty and correlation of the observed straight line segments.

The generality of the model makes it applicable to all problems containing homogeneous entities. With a small modification one can transfer it into a robust ML-estimation procedure, by iteratively reweighting the conditions g_i. Of course, due to the use of the redundant representation and the additional constraints, computation times are larger than when using specially adapted representations

because of the used overparametrization. But such a generic module for estimating with homogeneous entities may be used for rapid prototyping and for not too large problems in case computing time is not critical.

References

1. Matei, B., Meer, P.: A General Method for Errors–in–Variables Problems in Computer Vision. In: Computer Vision and Pattern Recognition Conference. Volume II., IEEE (June 2000) 18–25
2. Heuel, S.: Uncertain Projective Geometry. Statistical Reasoning in Polyhedral Object Reconstruction. Volume 3008 of Lecture Notes in Computer Science. Springer (2004)
3. Utcke, S.: Grouping based on Projective Geometry Constraints and Uncertainty. In Ahuja, N., Desai, U., eds.: Proceedings of the Sixth International Conference on Computer Vision, Bombay, India, Narosa Publishing House (January 4-7 1998) 739–746
4. Criminisi, A.: Accurate Visual Metrology from Single and Multiple Uncalibrated Images. Distinguished Dissertations. Springer, London, Berlin, Heidelberg (August 2001)
5. Clarke, J.C.: Modelling Uncertainty: A Primer. Technical Report 2161/98, Department of Engineering Science, University of Oxford (1998)
6. Chojnacki, W., Brooks, M.J., van den Hengel, A.: Rationalising the Renormalisation Method of Kanatani. Journal of Mathematical Imaging and Vision **14** (2001) 21–38
7. Kanatani, K.: Statistical Analysis of Geometric Computation. CVGIP: Image Understanding **59**(3) (May 1994) 286–306
8. Meidow, J., Beder, C., Förstner, W.: Reasoning with Uncertain Points, Straight Lines, and Straight Line Segments in 2D. ISPRS Journal of Photogrammetry and Remote Sensing **64**(2) (2009) 125–139
9. Koch, K.R.: Parameter Estimation and Hypothesis Testing in Linear Models. 2nd edn. Springer, Berlin (1999)
10. Huber, P.J.: Robust Statistics. J. Wiley, New York (1981)
11. Hartley, R., Zisserman, A.: Multiple View Geometry in Computer Vision. Cambridge University Press, Cambridge (2000)
12. Georgescu, B.: Software for HEIV based estimation, binary version. Center of Advanced Information Processing, Robust Image Understanding Laboratory, Rutgers University, http://www.caip.rutgers.edu/riul/research/code/heiv/ (2002)
13. Fischler, M.A., Bolles, R.C.: Random Sample Consensus: A Paradigm for Model Fitting with Applications to Image Analysis and Automated Cartography. Communications of the Association for Computing Machinery **24**(6) (1981) 381–395
14. Förstner, W., Gülch, E.: A Fast Operator for Detection and Precise Location of Distinct Points, Corners and Circular Features. In: Proceedings of the ISPRS Intercommission Conference on Fast Processing of Photogrammetric Data, Interlaken. (June 1987) 281–305
15. Collins, R.T., Weiss, R.S.: Vanishing Point Calculation as a Statistical Inference on the Unit Sphere. In: International Conference on Computer Vision. (December 1990) 400–403